
Accounting for the diversity in stellar environments

Michael Küffmeier

KUEFFMEIER@NBI.KU.DK

Centre for Star and Planet Formation, Niels Bohr Institute and Natural History Museum of Denmark, University of Copenhagen, Øster Voldgade 5-7, DK-1350 Copenhagen K, Denmark

Troels Haugbølle

HAUGBOEL@NBI.KU.DK

Centre for Star and Planet Formation, Niels Bohr Institute and Natural History Museum of Denmark, University of Copenhagen, Øster Voldgade 5-7, DK-1350 Copenhagen K, Denmark

Åke Nordlund

AAKE@NBI.KU.DK

Centre for Star and Planet Formation, Niels Bohr Institute and Natural History Museum of Denmark, University of Copenhagen, Øster Voldgade 5-7, DK-1350 Copenhagen K, Denmark

Abstract

Stars and their corresponding protoplanetary disks form in diverse environments. To account for these natural variations, we investigate the formation process around nine solar mass stars with a maximum resolution of 2 AU in a Giant Molecular Cloud of $(40 \text{ pc})^3$ in volume by using the adaptive mesh refinement code RAMSES. The magnetohydrodynamic simulations reveal that the accretion process is heterogeneous in time, in space, and among protostars of otherwise similar mass. During the first roughly 100 kyr of a protostar evolving to about a solar mass, the accretion rates peak around 10^{-5} to $10^{-4} M_{\odot} \text{ yr}^{-1}$ shortly after its birth, declining with time after that. The different environments also affect the spatial accretion, and infall of material to the star-disk system is mostly through filaments and sheets. Furthermore, the formation and evolution of disks varies significantly from star to star. We interpret the variety in disk formation as a consequence of the differences in the combined effects of magnetic fields and turbulence that may cause differences in the efficiency of magnetic braking, as well as differences in the strength and distribution of specific angular momentum.

1. Introduction

Protoplanetary disks form around stars as a consequence of pre-stellar cores collapsing in filaments of Giant Molecular Clouds, which makes them the smallest entity in a hierarchy of scales. Length scales range from tens of parsecs for Giant Molecular Clouds to protoplanetary disk sizes of ~ 10 AU to ~ 100 AU. It is computationally very challenging to cover such a broad range of scales in a single simulation. Therefore, simulations of protostellar formation traditionally start from initial conditions representing a collapsing spherically symmetric cloud, as an approximation to the pre-stellar core (Machida et al., 2004; 2006; 2007;

Machida & Matsumoto, 2011; Joos et al., 2012; 2013; Tomida et al., 2010; 2013; Li et al., 2011; Seifried et al., 2011; 2012; Vaytet & Haugbølle, 2016). This approach allows detailed parameter studies, but neglecting the underlying turbulence in Giant Molecular Clouds and the potential interactions with the surroundings could potentially limit the applicability of such idealized initial conditions. Considering the dynamics of Giant Molecular Clouds, it is important to investigate how they affect the formation of protostars and protoplanetary disks. Given that most of the volume in the Giant Molecular Cloud is of relatively low density and thus of less interest for star formation, simulating the huge range of scales becomes feasible by applying adaptive mesh refinement to the problem. First, we briefly explain the concept behind our zoom-method, which allowed us to resolve the accretion and disk formation process, while simultaneously accounting for the large-scale environment. Second, we present an overview of the most significant results obtained in our study before we discuss and summarize their consequences.

We use a highly modified version of the adaptive mesh-refinement code RAMSES (Teyssier, 2002; Fromang et al., 2006), which in principle can handle refinement over up to 29 factors of two (Nordlund et al., 2014). In Fig. 1, we sketch the procedure and refer the reader to (Kuffmeier et al., 2016; 2017a;b) for further details.

We start from an already turbulent GMC model of a cubic box of size $(40 \text{ pc})^3$ with periodic boundary conditions, consisting of self-gravitating, magnetized gas. The average H_2 number density is 30 cm^{-3} , which yields a total mass of the box of approximately $10^5 M_{\odot}$. The assumed GMC lifetimes are in agreement with the 'star formation in a crossing time' paradigm (Elmegreen, 2000; Elmegreen & Shadmehri, 2003; Padoan et al., 2016), and with observational estimates (Murray, 2011), and the turbulence is driven by massive stars that inject energy of 10^{51} erg of ther-

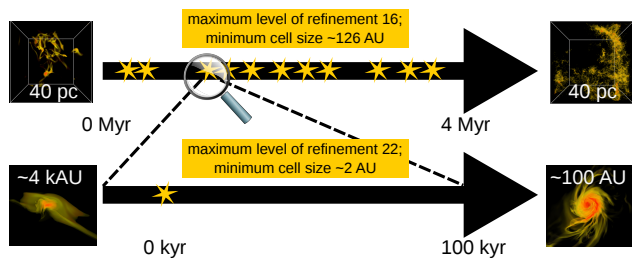


Figure 1. Sketch of the zoom-in procedure. First we evolve a snapshot of an already turbulent GMC of $(40 \text{ pc})^3$ in size (upper left image) for about 4 Myr (upper right image). During the evolution multiple sinks are created and at the current time more than 500 stars have formed. We zoom in on selected pre-stellar cores (lower left image) to resolve the formation process with higher resolution for up to about 100 kyr after sink creation (lower right image). This procedure is applied to altogether nine protostars.

mal energy into the GMC after a mass-dependent lifetime. For the heating via UV-photons (Osterbrock & Ferland, 2006), we apply the recipe of (Franco & Cox, 1986) and use an optically thin cooling function (Gnedin & Hollon, 2012) for the cold dense gas.

The combined effects of turbulence and self-gravity induce the formation of filaments, and subsequently star formation inside the filaments. To make the problem computationally tractable, we describe the collapse of matter into stars with a sub-grid sink particle algorithm. As illustrated in Fig. 1, we first evolve the GMC with a minimum cell size of 126 AU before we zoom-in onto the individual sinks of interest with a minimum cell-size of 2 AU. This second stage provides information about protostellar accretion, including the subsequent formation of protoplanetary disks.

2. Results of the zoom-ins

The different environments of the protostars cause differences in the accretion process and disk formation among the protostars. We illustrate the accretion profiles of nine sinks in the lower panel of Fig. 2. One can see a general trend for the different sinks, with a very steep initial increase to values of about $10^{-4} M_{\odot} \text{ yr}^{-1}$ to $10^{-5} M_{\odot} \text{ yr}^{-1}$ followed by a general decrease. The decrease varies between sinks and some of the sinks still show accretion rates of more than $10^{-6} M_{\odot} \text{ yr}^{-1}$ after ~ 100 kyr. Moreover, we can see that some of the sinks show significant fluctuations during their evolution. Since we average over periods of 200 to 400 years between the snapshots we are underestimating the amplitude of these episodic accretion events. Finally, we note that the sinks accrete their mass through accretion channels (Seifried et al., 2013) rather than uni-

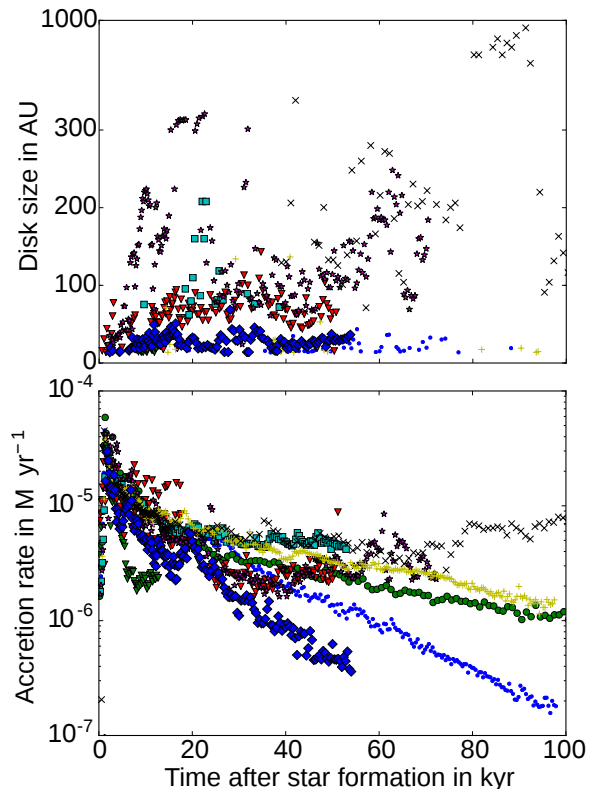


Figure 2. Upper panel: Evolution of the disk radius around the different sinks. Lower panel: Accretion profile for 9 sinks created in zoom-ins started with increased resolution before sink creation.

formly in space.

Fig. 3 shows slices in the plane perpendicular to the mean angular momentum vector at $t = 50$ kyr around six sinks. The images and the upper panel in Fig. 2 reveal the variety in disk formation for the different stellar environments, and also the spatial variations in the accretion process induced by filamentary arms feeding the forming protoplanetary disk. Also, the disks show signs of spiral arms or inflowing gas streams strikingly similar to what has been observed by ALMA and with the Subaru Next Generation Adaptive Optics (HiCIAO) (Liu et al., 2016).

3. Discussion and Conclusion

Using a numerical model that simultaneously encompass the large-scale environment of a Giant Molecular Cloud and the the immediate environment of nine protostars, covering seven orders of magnitude in dynamic range, we have investigated the environmental effects on the protostellar formation process. One major result is that stellar accretion can be very different

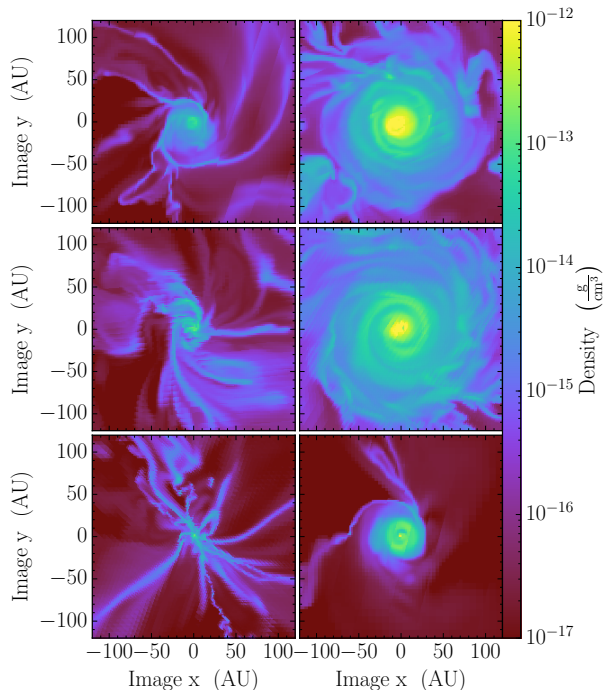


Figure 3. Slices in the plane vertical to the mean angular momentum vector calculated for a sphere of 100 AU around six different sinks at $t = 50$ kyr. The upper left slice corresponds to the sink with the blue dots in the accretion plot, the upper right to the red triangles, the middle left to the cyan squares, the middle right to the magenta asterisks, the lower left to the yellow pluses, and the lower right to the blue diamonds.

depending on the protostellar environment. We also conclude that the diversity in the large-scale stellar environment profoundly influences the formation and evolution of protoplanetary disks.

If the magnetization of the surrounding gas is sufficiently limited to avoid the magnetic braking catastrophe, protoplanetary disks of several tens of AU can form as early as a few thousand years after star formation. In cases where the magnetization of the collapsing gas is sufficiently large (low mass-to-flux ratios), no disk of more than ≈ 10 AU in size will form around the star. The main reason why the magnetic braking catastrophe is avoided in many cases is the reduction of magnetic braking caused by turbulence.

Acknowledgments

This research was supported by a grant from the Danish Council for Independent Research to ÅN, a Sapere Aude Starting Grant from the Danish Council for Independent Research to TH. Research at Centre for Star

and Planet Formation is funded by the Danish National Research Foundation (DNRF97). We acknowledge PRACE for awarding us access to the computing resource CURIE based in France at CEA for carrying out part of the simulations. Archival storage and computing nodes at the University of Copenhagen HPC center, funded with a research grant (VKR023406) from Villum Fonden, were used for carrying out part of the simulations and the post-processing. Finally, we acknowledge the developers of the python-based analyzing tool yt (<http://yt-project.org/>) (Turk et al., 2011) that simplified our analysis.

References

- Elmegreen, B. G. 2000, *ApJ*, 530, 277
- Elmegreen, B. G., & Shadmehri, M. 2003, *MNRAS*, 338, 817
- Franco, J., & Cox, D. P. 1986, *PASP*, 98, 1076
- Fromang, S., Hennebelle, P., & Teyssier, R. 2006, *A&A*, 457, 371
- Gnedin, N. Y., & Hollon, N. 2012, *ApJS*, 202, 13
- Joos, M., Hennebelle, P., & Ciardi, A. 2012, *A&A*, 543, A128
- Joos, M., Hennebelle, P., Ciardi, A., & Fromang, S. 2013, *A&A*, 554, A17
- Kuffmeier, M., Frostholm Mogensen, T., Haugbølle, T., Bizzarro, M., & Nordlund, Å. 2016, *ApJ*, 826, 22
- Kuffmeier M., Haugbølle T., Nordlund Å. 2017a, *ApJ*, 846, 7
- Kuffmeier M., Frimann S., Jensen S. S., Haugbølle T., 2017b, *ArXiv e-prints*, arXiv:1710.00931
- Larson, R. B. 1981, *MNRAS*, 194, 809
- Li, Z.-Y., Krasnopolsky, R., & Shang, H. 2011, *ApJ*, 738, 180
- Liu, H. B., Takami, M., Kudo, T., et al. 2016, *Science Advances*, 2, <http://advances.sciencemag.org/content/2/2/e1500875.full.pdf>
- Machida, M. N., Inutsuka, S.-i., & Matsumoto, T. 2007, *ApJ*, 670, 1198
- Machida, M. N., & Matsumoto, T. 2011, *MNRAS*, 413, 2767
- Machida, M. N., Matsumoto, T., Hanawa, T., & Tomisaka, K. 2006, *ApJ*, 645, 1227
- Machida, M. N., Tomisaka, K., & Matsumoto, T. 2004, *MNRAS*, 348, L1
- Murray, N. 2011, *ApJ*, 729, 133
- Nordlund, Å., Haugbølle, T., Kuffmeier, M., Padoan, P., & Vasileiades, A. 2014, in *IAU Symposium*, Vol. 299, *IAU Symposium*, ed. M. Booth, B. C. Matthews, & J. R. Graham, 131–135
- Osterbrock, D. E., & Ferland, G. J. 2006, *Astrophysics of gaseous nebulae and active galactic nuclei*

- Padoan, P., Pan, L., Haugbølle, T., & Nordlund, Å. 2016, *ApJ*, 822, 11
- Seifried, D., Banerjee, R., Klessen, R. S., Duffin, D., & Pudritz, R. E. 2011, *MNRAS*, 417, 1054
- Seifried, D., Banerjee, R., Pudritz, R. E., & Klessen, R. S. 2013, *MNRAS*, 432, 3320
- Seifried, D., Pudritz, R. E., Banerjee, R., Duffin, D., & Klessen, R. S. 2012, *MNRAS*, 422, 347
- Teyssier, R. 2002, *A&A*, 385, 337
- Tomida, K., Tomisaka, K., Matsumoto, T., et al. 2013, *ApJ*, 763, 6
- . 2010, *ApJ*, 714, L58
- Turk, M. J., Smith, B. D., Oishi, J. S., et al. 2011, *ApJS*, 192, 9
- Vaytet, N., & Haugbølle, T. 2016, *A&A*, 598, A116